Characterization of AJH-836, a diacylglycerol-lactone with selectivity for novel PKC isozymes

Received for publication, October 2, 2017, and in revised form, March 8, 2018 Published, Papers in Press, April 10, 2018, DOI 10.1074/jbc.RA117.000235

Mariana Cooke[‡], Xiaoling Zhou[§], Victoria Casado-Medrano[‡], Cynthia Lopez-Haber[‡], Martin J. Baker[‡], Rachana Garg[‡], Jihyae Ann[¶], Jeewoo Lee[¶], Peter M. Blumberg[§], and Marcelo G. Kazanietz[‡1]

From the [‡]Department of Systems Pharmacology and Translational Therapeutics, Perelman School of Medicine, University of Pennsylvania, Philadelphia, Pennsylvania 19104-6160, [§]Laboratory of Cancer Biology and Genetics, Center for Cancer Research, NCI, National Institutes of Health, Bethesda, Maryland 20892, and [¶]Laboratory of Medicinal Chemistry, College of Pharmacy, Seoul National University, Seoul 08826, Republic of Korea

Edited by Eric R. Fearon

Diacylglycerol (DAG) is a key lipid second messenger downstream of cellular receptors that binds to the C1 domain in many regulatory proteins. Protein kinase C (PKC) isoforms constitute the most prominent family of signaling proteins with DAG-responsive C1 domains, but six other families of proteins, including the chimaerins, Ras-guanyl nucleotide–releasing proteins (RasGRPs), and Munc13 isoforms, also play important roles. Their significant involvement in cancer, immunology, and neurobiology has driven intense interest in the C1 domain as a therapeutic target. As with other classes of targets, however, a key issue is the establishment of selectivity. Here, using [^{3}H]phorbol 12,13-dibutyrate ([^{3}H]PDBu) competition binding assays, we found that a synthetic DAG-lactone, AJH-836, preferentially binds to the novel PKC isoforms PKCδ and PKCϵ relative to classical PKCα and PKCβII. Assessment of intracellular translocation, a hallmark for PKC activation, revealed that AJH-836 treatment stimulated a striking preferential redistribution of PKCϵ to the plasma membrane relative to PKCα. Moreover, unlike with the prototypical phorbol ester phorbol 12-myristate 13-acetate (PMA), prolonged exposure of cells to AJH-836 selectively down-regulated PKCδ and PKCϵ without affecting PKCα expression levels. Biologically, AJH-836 induced major changes in cytoskeletal reorganization in lung cancer cells, as determined by the formation of membrane ruffles, via activation of novel PKCs. We conclude that AJH-836 represents a C1 domain ligand with PKC-activating properties distinct from those of natural DAGs and phorbol esters. Our study supports the feasibility of generating selective C1 domain ligands that promote novel biological response patterns.

This work was supported by National Institutes of Health Grants ES026023, CA189765, and CA196232 (to M. G. K.); by National Research Foundation of Korea for the Global Core Research Center Grant 2011-0030001; and in part by the Intramural Research Program of the National Institutes of Health, Center for Cancer Research, NCI Project Z1A BC 005270. The authors declare that they have no conflicts of interest with the contents of this article. The content is solely the responsibility of the authors and does not necessarily represent the official views of the National Institutes of Health.
This article contains Fig. S1.

[1] To whom correspondence should be addressed: Dept. of Systems Pharmacology and Translational Therapeutics, Perelman School of Medicine, University of Pennsylvania, 1256 Biomedical Research Bldg. II/III, 421 Curie Blvd., Philadelphia, PA 19104-6160. Tel.: 215-898-0253; Fax: 215-746-8941; E-mail: marcelog@upenn.edu.

Lipid second messengers, in particular diacylglycerol (DAG)[2] and phosphoinositides, have emerged as key signaling molecules downstream of innumerable cellular receptors. Responses to DAG are mediated by seven families of proteins, protein kinase C (PKC), chimaerin, RasGRP, protein kinase D, MRCK, Munc13, and DAG kinase, which combine a DAG recognition motif, termed a (typical) C1 domain, along with disparate functional domains and other regulatory domains. Among these families of signaling proteins, the PKC isoforms have been studied most intensely (1–3).

PKC isozymes are key elements in signaling cascades that control multiple cellular functions, including proliferation, survival, motility, and gene expression, and have been widely implicated in cancer progression and other diseases. Of the 10 human PKC isoforms, both the "classical/conventional" (cPKCs) (α, βI, βII, and γ) and "novel" PKCs (nPKCs) (δ, ϵ, η, and θ) contain twin C1 domains that recognize DAG, whereas only the cPKCs contain a C2 domain that responds to elevated internal calcium. For both C1 and C2 domains, ligand binding leads to insertion/bridging of the C1/C2 domains to the membrane with formation of the ternary complex of domain, ligand, and phospholipid. Typically, there is a requirement for acidic phospholipids such as phosphatidylserine for this membrane interaction (3–5).

Phorbol esters have become the most extensively characterized nonphysiological natural compounds capable of activating PKCs. These diterpenes bind with high affinity to the C1 domains located in the N-terminal regulatory domain of cPKCs and nPKCs, competing with DAG for binding to C1 domains (6, 7). The C1 domains from PKCs and other proteins with phorbol ester/DAG–binding capabilities possess an overall similar globular structure, stabilized by twin zinc fingers, with the phorbol ester/DAG–binding site formed from a hydrophilic cavity bounded by a hydrophobic rim. Phorbol ester/DAG binding completes the hydrophobic surface, while the specific substituents on the phorbol ester/DAG contribute further hydrophobic character. The increased hydrophobicity drives/

[2] The abbreviations used are: DAG, diacylglycerol; RasGRP, Ras-guanyl nucleotide–releasing protein; PDBu, phorbol 12,13-dibutyrate; PMA, phorbol 12-myristate 13-acetate; cPKC, classical/conventional PKC; nPKC, novel PKC; NSCLC, non-small-cell lung cancer; TAT, transactivator of transcription.

stabilizes insertion of the C1 domain–ligand complex into the membrane lipid bilayer. This insertion is further stabilized by interactions between charged residues on the surface of the C1 domain with acidic phospholipid headgroups (8, 9). The redistribution to membranes induced by phorbol esters or related C1 domain ligands, *i.e.* the translocation from the cytosolic compartment to the plasma membrane or internal membranes, is a hallmark of PKC activation and can be readily visualized in cellular models by using fluorescently tagged PKCs (10, 11).

As might be anticipated from their central role in cellular signaling, the signaling network downstream from the PKC isoforms and the other families of signaling proteins with typical C1 domains is extraordinarily complex. Thus, individual PKC isoforms have been shown to confer distinctive patterns of cellular responses, and the differences between isoforms may be dramatic. Depending on cellular context, PKCα, PKCδ, and PKCϵ, the most commonly expressed PKCs, can trigger mitogenic/tumor-promoting or conversely antimitogenic/tumor suppressor responses (3, 12, 13). A prediction is that ligands binding to typical C1 domains with differential selectivity could therefore induce distinct patterns of biological response.

Although the relevant mechanisms may be uncertain, there are clear examples of C1 domain–targeted ligands inducing distinct patterns of response. Whereas phorbol 12-myristate 13-acetate (PMA) is the archetypical mouse skin tumor promoter, prostratin (12-deoxyphorbol 13-acetate) was shown to be anti-tumor promoting. Bryostatin 1, a DAG-mimetic macrocyclic polyacetate, activates PKCs *in vitro* but paradoxically antagonizes many phorbol ester responses. Ingenol 3-angelate only partially stabilizes PKC–membrane interactions. Such diversity of response underlies therapeutic potential. Ingenol 3-angelate (under the trade name Picato^{TM}) has been approved for treatment of actinic keratosis. Bryostatin 1 has been the subject on numerous clinical trials for cancer and more recently for dementia. Prostratin has been proposed as an agent for conferring sensitivity to drug treatment for cells latently bearing HIV (12, 14–17).

A daunting challenge in the development of inhibitors for kinases has proven to be the large size of the kinome and the high homology in the ATP-binding site in the kinase domain (12, 18). Although the high structural similarities among the binding clefts of C1 domains might *a priori* suggest similar problems, several factors provide encouragement. Most importantly, natural products such as prostratin, bryostatin 1, and ingenol 3-angelate have unambiguously proven that C1-targeted ligands can achieve differential biological outcomes (12–18). Deeper consideration of the mechanism provides a rationale. First, the ligand forms a ternary complex of C1 domain–ligand inserted into the lipid bilayer. The interaction surface of this complex is thus much more extensive than simply that formed between the ligand and the binding cleft of the C1 domain, and there are extensive differences in the surfaces of the typical C1 domains that interact with the lipid headgroups. Second, it is appreciated that different ligands can cause different depths of insertion, changing these interactions. Furthermore, there is considerable diversity between cellular membranes or between microdomains within the membrane, changing the lipid environment with which the interactions will take place (5, 12, 19, 20).

A powerful approach for generating structural diversity among C1 domain–targeted ligands has been through a DAG-lactone template, affording compounds approaching the phorbol esters in potency (19–23). Cyclization of DAGs to rigid lactone structures reduces the entropic penalty associated with the flexibility of the glycerol backbone and provides a scaffold with rich opportunities for decoration at positions homologous to the side chains of DAG. The power of this approach has been shown in the analysis of combinatorial libraries of DAG-lactones where changes in the patterns of acyl and alkyl substitution yielded marked differences in the patterns of biological outcome (24). Likewise, targeted synthesis of DAG-lactones, extending insights from the combinatorial chemistry, have yielded compounds with marked selectivity for the RasGRP family of C1 domain–containing signaling proteins relative to their affinity for PKC (20).

It has been previously reported that natural DAGs bind with similar affinities to all cPKCs and nPKCs (25). Toward the objective of generating isozyme-specific PKC ligands, Ann *et al.* (26) had described the incorporation of linoleic acid derivatives as well as saturated and unsaturated alkyl chains into the side chains of DAG-lactones and characterized these derivatives for their *in vitro* binding affinity toward PKCϵ, an oncogenic member of the PKC family, relative to PKCα (27–32). Following up on this analysis, here we describe that the DAG-lactone AJH-836 showed marked selectivity for PKCϵ and PKCδ relative to PKCα in multiple cell types, unlike the typical phorbol ester PMA, and correspondingly displayed a distinct pattern of biological activity. The pattern of selectivity among PKC isoforms of AJH-836 is novel, further emphasizing the rich opportunities afforded by C1 domain–targeted ligands.

Results

Differential in vitro binding of AJH-836 to PKC isozymes

Extensive synthetic efforts have generated DAG-lactones substituted with a diversity of saturated and unsaturated alkyl and aryl chains at the *sn*-1 and *sn*-2 positions on the DAG-lactone (21, 26). In binding studies using a lipid mixture designed to mimic nuclear membranes (23), the DAG-lactone (*E*)-(2-(hydroxymethyl)-4-(3-isobutyl-5-methylhexylidene)-5-oxotetrahydrofuran-2-yl)methyl pivalate (referred to here as AJH-836; Fig. 1*A*) was found to display some specificity toward the novel PKCϵ relative to the classical PKCα, although the assay conditions were not fully comparable (26). For comparison, no specificity was observed under these conditions for the DAG-lactone (*Z*)-(2-(hydroxymethyl)-4-(3-methylbutylidene)-5-oxotetrahydrofuran-2-yl)methyl octadeca-9,11-diynoate (referred to here as AJH-1512; Fig. 1*A*) (26).

Here, our initial objective was to examine the ability of AJH-836 to bind to recombinant PKCα, PKCβII, PKCδ, and PKCϵ (four of the main phorbol ester–responsive PKCs expressed in cancer cells) under parallel conditions using a competition [20-^{3}H]phorbol 12,13-dibutyrate ([^{3}H]PDBu) binding assay with phosphatidylserine vesicles as cofactor (5). Under these condi-

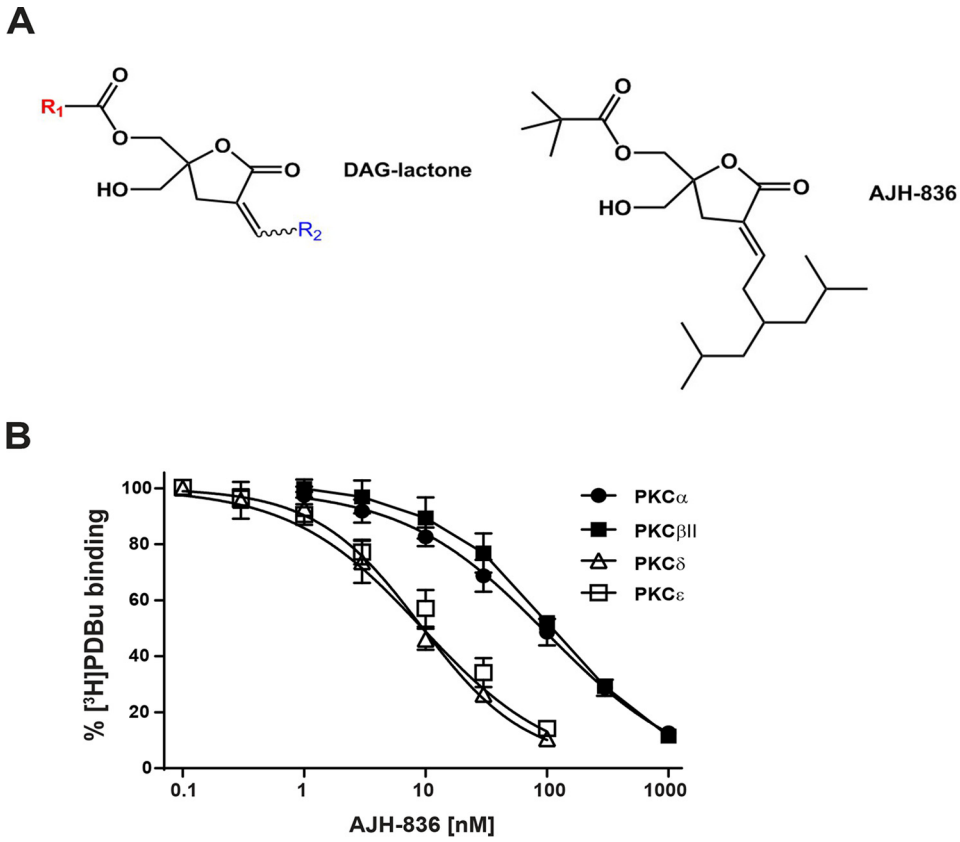

Figure 1. *In vitro* binding of AJH-836 to PKCα, PKCδ, and PKCϵ. *A*, general structures of DAG-lactones (*left*) and AJH-836 (*right*). *B*, binding was performed by competition of a fixed concentration of [^{3}H]PDBu (~1.3 nM) in the presence of 100 μg/ml phosphatidylserine, 1 mM EGTA, and increasing concentrations of nonradioactive AJH-836. The K_i values are presented in Tables 1 and 2. Results are expressed as mean ± S.E. (*error bars*) ($n = 3$).

tions, AJH-836 preferentially bound the novel PKC isoforms PKCϵ and PKCδ with ~10–12-fold higher affinity relative to the classical PKC isoforms PKCα and PKCβII (Fig. 1*B* and Tables 1 and 2). In contrast, AJH-1512 (23) showed similar affinities for all four isoforms (Tables 1 and 2).

Differential translocation of PKCα and PKCϵ by AJH-836 in cellular models

In vitro binding assays using reconstituted phospholipid vesicles will necessarily fail to capture the full range of differences in C1 domain ligand recognition occurring in a cellular context. To tackle this issue, we next examined subcellular translocation of the individual PKC isoforms expressed in cells as GFP-fused proteins. We hypothesized that the differential binding properties observed *in vitro* for AJH-836 and AJH-1512 could be reflected in characteristic patterns of PKC isozyme translocation in cellular models.

Treatment of HeLa cervical adenocarcinoma cells with AJH-836 fully translocated PKCϵ to the plasma membrane in a concentration-dependent manner (Fig. 2*A*). The EC_{50} for this effect was 0.23 μM. Conversely, much higher AJH-836 concentrations were required to induce PKCα plasma membrane translocation (EC_{50} = 9.8 μM). The ratio EC_{50} PKCα/EC_{50} PKCϵ of 43 indicates a notable selectivity for activation of PKCϵ by AJH-836 in this cellular context. Unlike AJH-836, AJH-1512 displayed similar potencies for translocation of these PKCs (EC_{50} PKCα = 26.1 μM; EC_{50} PKCϵ = 17.1 μM; ratio EC_{50} PKCα/EC_{50} PKCϵ = 1.5) (Fig. 2*B*), which was consistent with the lack of selectivity observed in *in vitro* binding assays. As a control, PMA, which potently activates cPKCs and nPKCs, fully translocated both PKCα and PKCϵ to the plasma membrane.

Although PKCα is the major classical PKC isoform in HeLa cervical adenocarcinoma cells, PKCδ is the second major, well-studied novel PKC isoform along with PKCϵ in these cells (33). Because our *in vitro* binding assays revealed similar preferential

Table 1
DAG-lactone binding affinities for PKCα, PKCβII, PKCδ, and PKCϵ *in vitro*
Values represent the mean ± S.E. of three independent experiments and were calculated from the ID_{50} values determined from the competition curves as described under "Experimental procedures."

PKC isoform	K_i	
	AJH-836	AJH-1512
	nM	
PKCα	23.6 ± 2.0	25.1 ± 1.7
PKCβII	19.7 ± 0.8	16. 5 ± 0.3
PKCδ	1.89 ± 0.16	8.78 ± 0.96
PKCϵ	1.89 ± 0.20	15.7 ± 1.1

Table 2
K_i ratios for DAG-lactones AJH-836 and AJH-1512

Compound	K_i ratio	
	PKCα/nPKC	PKCβII/nPKC
AJH-836	PKCα/PKCδ = 12.4 PKCα/PKCϵ = 12.4	PKCβII/PKCδ = 10.4 PKCβII/PKCϵ = 10.4
AJH-1512	PKCα/PKCδ = 2.9 PKCα/PKCϵ = 1.6	PKCβII/PKCδ = 1.9 PKCβII/PKCϵ = 1.1

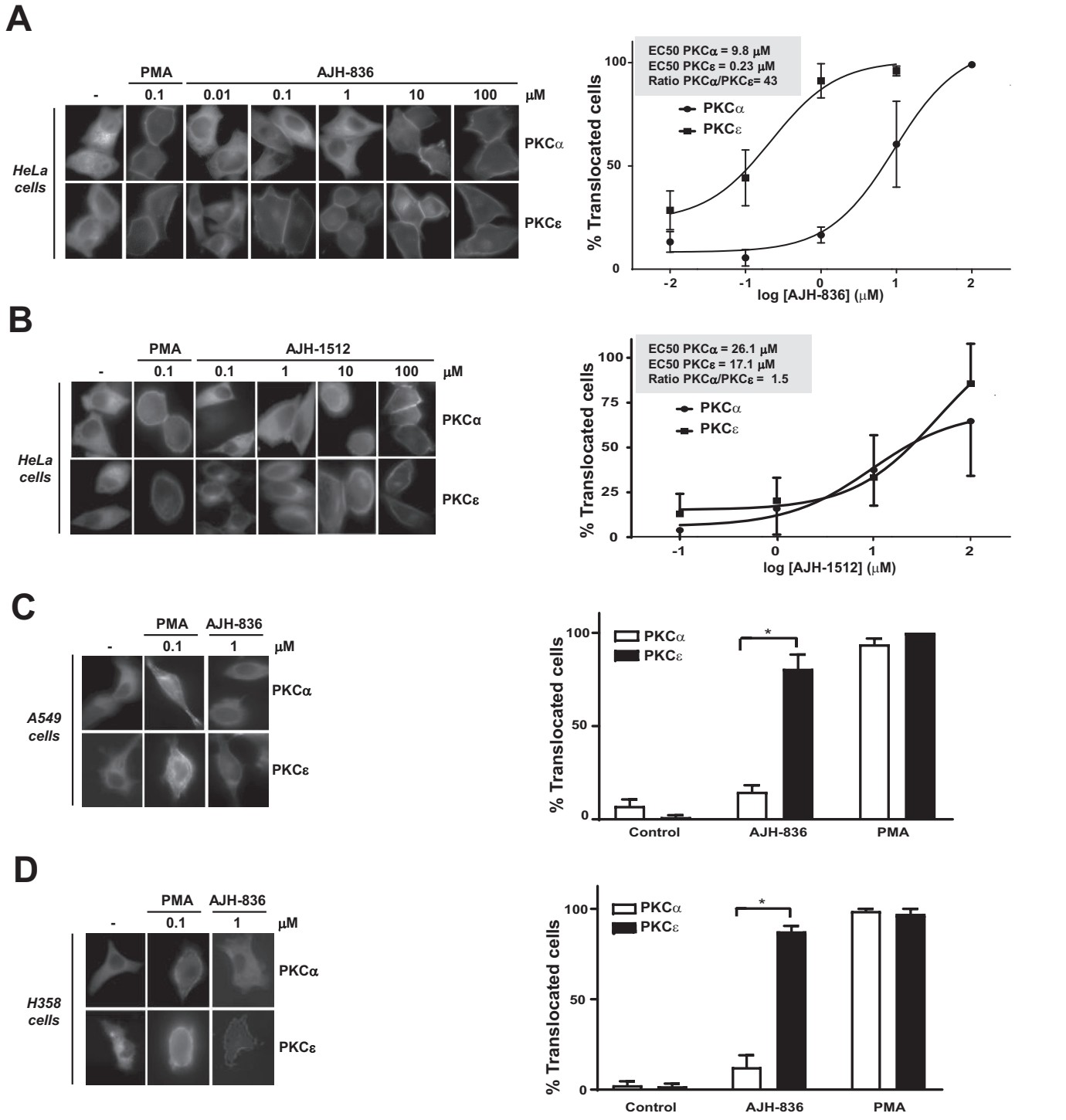

Figure 2. Differential translocation of PKCs by AJH-836 in cellular models. Cells were transfected with pEGFP-PKCα or pEGFP-PKCε plasmids and 24 h later serum-starved for an additional 24 h. Cells were then stimulated for 30 min with PMA, AJH-836, AJH-1512, or vehicle as indicated in each case; fixed; and visualized by fluorescence microscopy. *A*, dose dependence of PKCα and PKCε intracellular translocation in HeLa cells by AJH-836. *B*, dose dependence of PKCα and PKCε intracellular translocation in HeLa cells by AJH-1512. *C*, effect of AJH-836 and PMA on PKCα and PKCε translocation in A549 cells. *D*, effect of AJH-836 and PMA on PKCα and PKCε translocation in H358 cells. *Left*, representative micrographs are shown. *Right*, quantification of translocated cells. For each condition, 20–100 cells were counted. Results are expressed as mean ± S.E. (*error bars*) of three to five individual experiments. *Inset*, EC_{50} for translocation and EC_{50} ratio. *, $p < 0.001$.

affinities for PKCε and PKCδ for AJH-836, we wished to address whether this DAG-lactone displays similar selectivity for PKCδ translocation in the cellular context. A limitation, however, is the predominant pattern of PKCδ translocation to internal membranes (perinuclear/Golgi region and nuclear membrane) (11, 22, 34–36), which makes it less objective to quantify upon direct visualization. Moreover, prominent perinuclear PKCδ localization could be observed under basal conditions in HeLa cells (Fig. S1). As expected, AJH-836 treatment led to a quite heterogeneous pattern of PKCδ translocation with

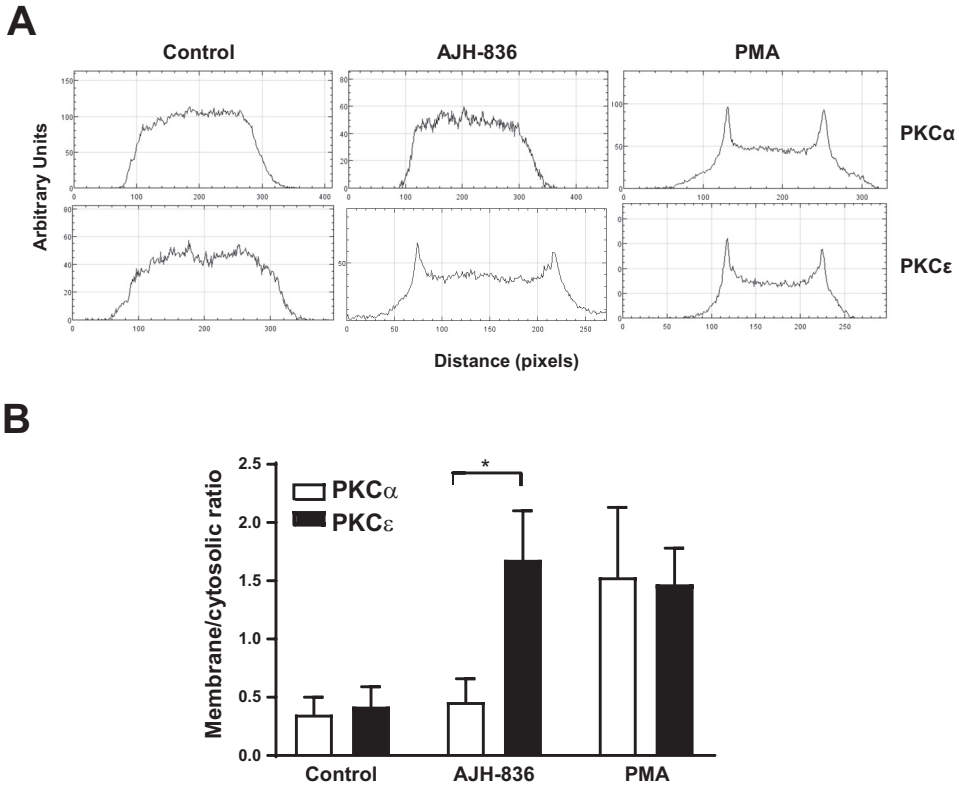

Figure 3. Quantification of plasma membrane translocation of PKCα and PKCϵ by AJH-836 treatment. HeLa cells were transfected with pEGFP-PKCα or pEGFP-PKCϵ plasmids and 24 h later serum-starved for an additional 24 h. Cells were then stimulated for 30 min with 1 μM AJH-836 or vehicle. As a positive control, 0.1 μM PMA was used. After fixation, cells were visualized by fluorescence microscopy. Quantification of membrane/cytosol ratio was done with ImageJ as described under "Experimental procedures." *A*, representative graphs. *B*, membrane/cytosol ratio was calculated for 100–150 individual cells in each group. Results are expressed as mean ± S.E. (*error bars*) *, $p < 0.001$.

cells showing staining in plasma membrane, nuclear membrane, and/or the perinucleus. If only plasma membrane translocation were assessed, results revealed a reduced ability of AJH-836 to redistribute PKCδ relative to PKCϵ (EC_{50} = 11 μM; ratio EC_{50} PKCδ/EC_{50} PKCϵ = 48) (data not shown).

As the pattern of PKC isozyme translocation may vary depending on the cellular context, we also evaluated PKCα and PKCϵ relocalization by AJH-836 in A549 and H358 non-small-cell lung cancer (NSCLC) cells. We used a concentration of AJH-836 of 1 μM, which showed the maximum difference in translocation between PKCα and PKCϵ in HeLa cells. As clearly shown in Fig. 2, *C* and *D*, AJH-836 fully translocated PKCϵ in both A549 and H358 NSCLC cells, whereas translocation of PKCα was negligible. As expected, PMA caused full translocation of both PKCα and PKCϵ to the plasma membrane in NSCLC cells.

To further corroborate the differential translocation pattern of PKC isozymes by AJH-836, we carried out a quantitative densitometric analysis of PKC cellular localization using ImageJ. As shown in Fig. 3, PMA promoted a marked shift in cytosolic to membrane intensity for both PKCα and PKCϵ in HeLa cells with a 4.4- and 4.0-fold increase in the membrane/cytosolic PKC ratio, respectively. In contrast, the pattern of redistribution of PKCα and PKCδ induced by AJH-836 was drastically different. Indeed, at 1 μM, AJH-836 treatment caused a 3.5-fold increase in the membrane/cytosolic ratio for PKCϵ, whereas it did not appreciably affect this ratio for PKCα, thus confirming the selectivity of this DAG-lactone for PKCϵ.

Activation of PKCδ by AJH-836 in cellular models

To investigate the potential ability of AJH-836 to activate PKCδ, we measured PKCδ phosphorylation at Ser^{299}. Phosphorylation at this site has been reported to be a marker of catalytically active enzyme (37, 38). Analysis of Ser^{299}-PKCδ phosphorylation by Western blotting using a specific phosphoantibody revealed concentration-dependent activation by AJH-836 in HeLa, A549, and H358 cells. Our results revealed maximum phosphorylation by AJH-836 at 10 μM in all cases. The EC_{50} values from the phospho-Ser^{299}-PKCδ densitometric analysis were 0.8 (HeLa cells), 1.3 (A549 cells) and 0.9 μM (H358 cells) (Fig. 4).

Differential down-regulation of PKC isozymes by prolonged treatment with AJH-836

Prolonged stimulation of cells with phorbol ester analogues is known to down-regulate the expression of PKCs, a process that occurs upon sustained association with the plasma membrane and is mediated via protein degradation at intracellular compartments (39–41). We compared the ability of AJH-836 to down-regulate the PKC isoforms as a function of time and concentration using the NSCLC cellular models. Down-regulation of PKCδ and PKCϵ by AJH-836 in the A549 and H358 cells was negligible after 3 h and began to be detected at 6 h, partic-

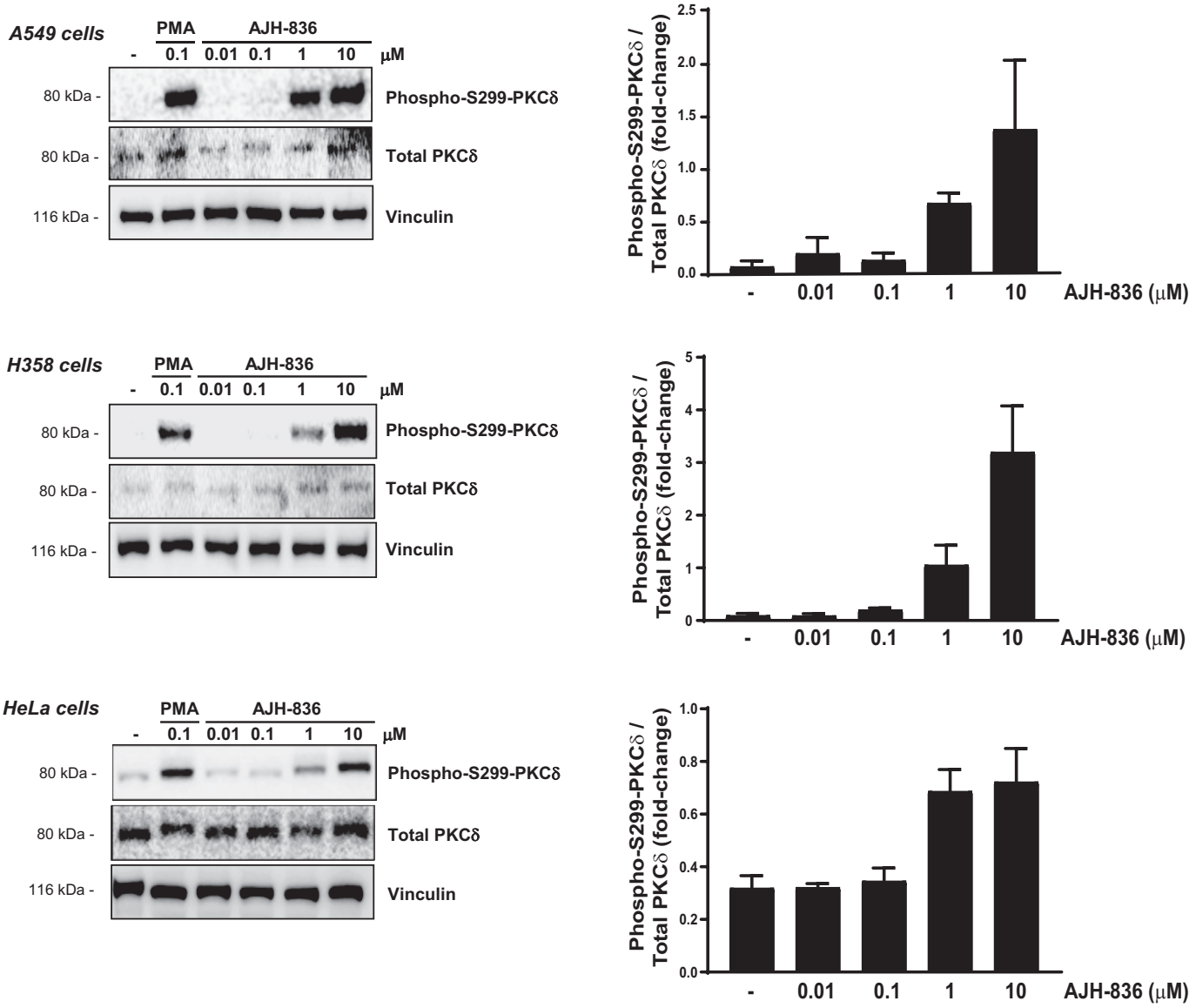

Figure 4. Activation of PKCδ by AJH-836. HeLa, A549, and H358 cells were stimulated for 5 min with different concentrations of AJH-836 or PMA as indicated. Phospho-Ser^{299}-PKCδ was determined by Western blotting. As loading controls, we used anti-PKCδ and anti-vinculin antibodies. *Upper panels*, representative Western blots. *Lower panels*, densitometric analysis of phospho-Ser^{299}-PKCδ signal relative to total PKCδ, expressed as relative to the PMA effect. Results are expressed as mean ± S.E. (*error bars*) of three individual experiments.

ularly at 1 μM AJH-836. Near complete down-regulation for both PKCδ and PKCε was observed after 16 or 24 h of treatment with 1 μM AJH-836 for both the A549 and H358 cells. In contrast, the pattern of PKCα down-regulation was notably different. PKCα levels in the A549 and H358 cells remained essentially unchanged upon treatment with 1 μM AJH-836, even at the longer time points. Only a partial PKCα down-regulation could be observed at the highest concentration used in this analysis (10 μM) (Fig. 5, *A* and *B*). The distinctive pattern of PKC isozyme down-regulation caused by AJH-836 became more evident when compared with that induced by PMA. PMA down-regulated all three PKC isoforms in the NSCLC cells with a slight preference toward PKCα. This differential sensitivity for PKC isozyme down-regulation between PMA and AJH-836 is depicted in Fig. 5, *C* and *D*.

AJH-836 induces major changes in cytoskeletal morphology

We have previously reported that specific activation of lung cancer cells with PMA induces the formation of lamellipodia and membrane ruffles, actin-rich cytoskeletal structures implicated in the reorganization of actin cytoskeleton and cell motility. This effect is mediated by the activation of the small G-protein Rac1. PKCε has been shown to be a crucial mediator of ruffle formation in lung cancer cells (31, 42, 43). To investigate the functional responses triggered by AJH-836, we examined morphological changes induced by this agent in A549 cells. Fig. 6*A* shows that the DAG-lactone induces the formation of ruffles in A549 cells in a concentration-dependent manner. Next, we examined the effect of PKC inhibitors with distinctive isozyme selectivity on the ability of AJH-836 to induce ruffles.

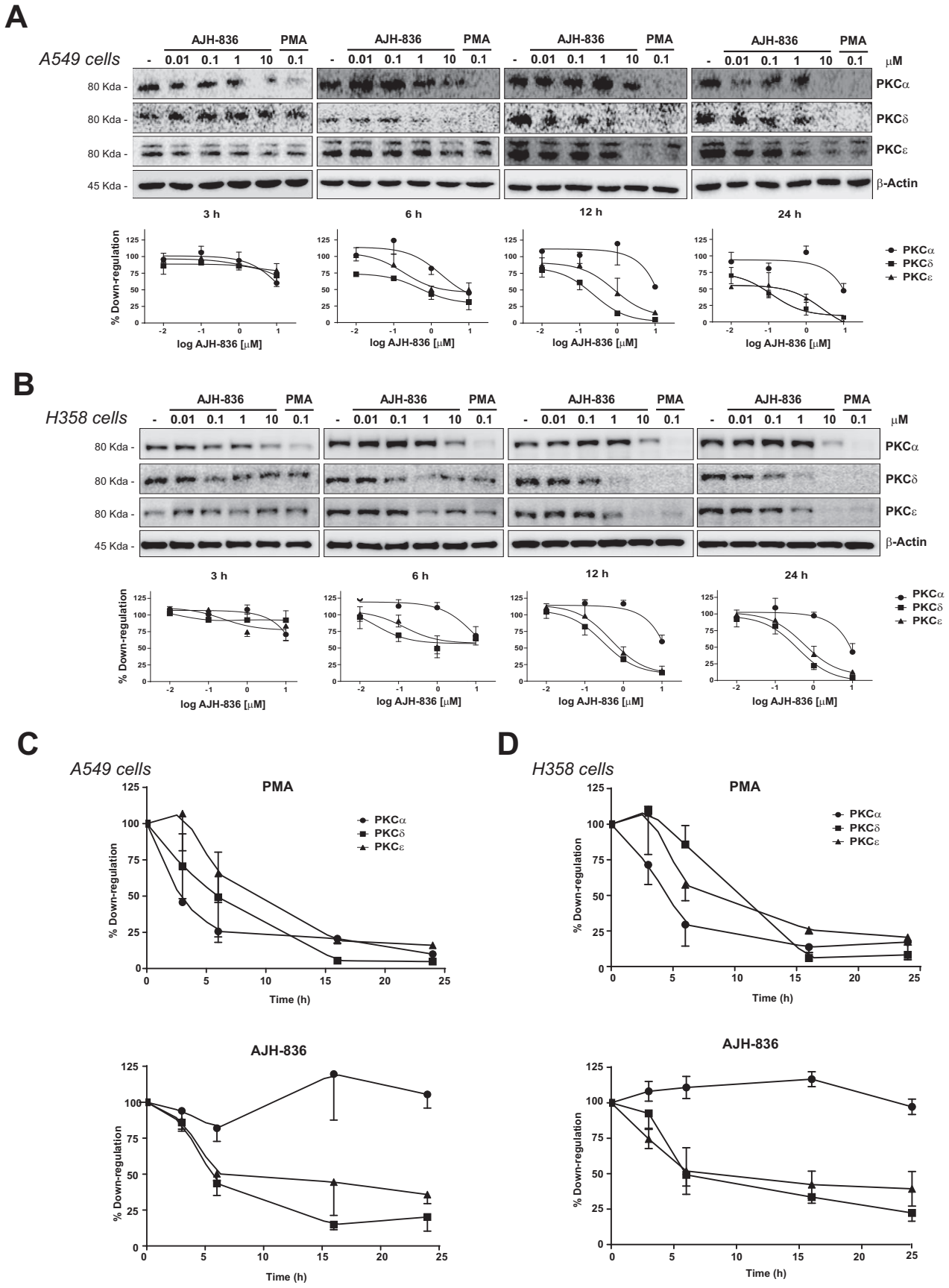
A
A549 cells
AJH-836
PMA
- 0.01 0.1 1 10 0.1
μM
80 Kda -
45 Kda -
PKCα
PKCδ
PKCε
β-Actin
3 h
6 h
12 h
24 h
% Down-regulation
log AJH-836 [μM]
B
H358 cells
C
A549 cells
PMA
AJH-836
Time (h)
D
H358 cells

The widely used pan-PKC inhibitors GF109203X and Gö6983, which inhibit both nPKCs and cPKCs, caused complete inhibition in ruffle formation induced by AJH-836. In contrast, Gö6976, which preferentially inhibits cPKCs over nPKCs (44), only caused a small reduction in ruffle formation (Fig. 6*B*).

To further assess the involvement of individual PKCs expressed in A549 cells in AJH-836–induced ruffle formation, we used validated RNA interference (RNAi) duplexes to knock down PKCα, PKCδ, or PKCε (Fig. 6*C*). Consistent with the involvement of PKCε in cytoskeleton rearrangement (31), silencing its expression caused a marked reduction in the formation of ruffles induced by the DAG-lactone. Conversely, no inhibition in AJH-836–induced ruffle formation could be observed upon silencing PKCα. PKCδ RNAi depletion in A549 cells caused a marginal reduction in ruffle formation by AJH-836, although not statistically significant ($p = 0.06$), and did not have any additive effect when knocked down together with PKCε.

Lastly, to further confirm the involvement of PKCε as a target for AJH-836 in A549 cells, we took advantage of εV1-2, a TAT-fused peptide that selectively inhibits PKCε (18, 30, 31, 45). This inhibitor caused a significant inhibition in ruffle formation induced by the DAG-lactone, whereas a TAT control peptide had no effect (Fig. 6*D*). Although we did not examine the activity of AJH-836 on targets other than the PKC isoforms, these experiments clearly show that the effects of AJH-836 on morphology in the cell systems examined were mediated by the novel PKCs, in particular PKCε.

Discussion

In the present study, we characterized a DAG analogue, AJH-836, which has higher affinity *in vitro* for novel PKCδ and PKCε isozymes relative to PKCα. Consistent with this result, analysis of intracellular relocalization revealed that AJH-836 has greater potency for translocation (*i.e.* activation) of PKCε to the plasma membrane relative to PKCα. This is quite remarkable because, as demonstrated in early studies, DAG generated physiologically upon activation of receptors displays similar *in vitro* affinities for cPKCs and nPKCs, a pattern also observed for prototypical phorbol esters. Unlike AJH-836, other DAG-lactones have been reported to have similar activities for cPKCs and nPKCs *in vitro* and better translocate PKCα to the plasma membrane (22, 46). Other natural compounds with C1 domain–binding capabilities such as 12-deoxyphorbol esters, mezerein, and thymeleatoxin have higher affinities for cPKCs relative to nPKCs (25).

It is well-established that phorbol esters and related analogues, including DAG-lactones, bind specifically to the C1 domains in cPKCs and nPKCs. These domains are duplicated in tandem (C1a and C1b) in these two PKC subfamilies. Binding occurs in the groove formed where the two strands of a β-sheet pull away from each other, and the bound ligand results in a completed hydrophobic surface on the C1 domains that is energetically favorable to interact with the hydrocarbon core of the phospholipid bilayer. Basic residues distal to the phorbol ester/DAG–binding site contribute by interacting with headgroups from acidic phospholipids (8). In a cellular context, phorbol ester/DAG binding to the C1 domain triggers the translocation of the enzyme to membranes. C1 domains also have additional roles, including binding to autoinhibitory sites, that reflect the potential differential roles of "exposed" *versus* "nonexposed" C1 domains (9, 47, 48). The differential binding of AJH-836 to PKCs may be the consequence of different scenarios, one of the obvious being the preferential association between the ligand and nPKC C1 domains dictated by specific residues interacting with the DAG-lactone backbone and/or alkyl chains in the appropriate binding modes. It is probable that specific "ternary complex" interactions that involve membrane phospholipids may contribute to AJH-836 isozyme specificity as well, a setting that is consistent with the dependence of its binding affinity on the membrane composition (26). Although dissecting the individual structural features contributing to the pattern of PKC isoform selectivity will depend on extensive structural analysis, the current data make unambiguously clear that it is possible to generate differential PKC isoform selectivity such as described here along with differential biology.

AJH-836 is structurally simple compared with the highly complex natural PKC ligands such as the phorbol esters, bryostatins, ingenols, and indolactams. It therefore provides a powerful lead compound for probing the features conferring nPKC selectivity. Structure–activity analysis based on modifications of DAG-lactones has proven to be a successful approach for the generation of potent analogues capable of distinguishing between different proteins with C1 domains (20, 25, 49, 50), and it therefore represents a promising strategy for achieving PKC isozyme selectivity. It should be emphasized that absolute selectivity among the families and family members of the signaling proteins that contain typical C1 domains is not necessary to generate useful compounds. Rather, as evidenced by natural products such as bryostatin 1, ingenol 3-angelate, and prostratin, compounds that can generate different patterns from the rich network of responses downstream of these signaling proteins may have utility.

One attractive scenario where selective agents such as AJH-836 may have unique effects is in cancer cell models where individual PKCs seem to exert specific functions. For example, PKCε is largely overexpressed in epithelial cancer cell lines and drives migratory and metastatic phenotypes (3, 27, 29–32). In this context, we found that AJH-836 promotes the formation of ruffles, a step that is essential for cancer cell motility. Because PKCε has tumor-promoting functions and other PKCs, including PKCα, have been shown to suppress tumor growth (3, 27), differential regulation of PKC isoforms such as PKCε and PKCα

Figure 5. Differential down-regulation of PKC isozymes by AJH-836. Cells were serum-starved for 24 h and then treated with different concentrations of AJH-836 (0.01–10 μM) or PMA (0.1 μM). Cells were lysed at different time points (3, 6, 16, and 24 h), and expression of endogenous PKC isozymes was determined by Western blotting using antibodies against specific PKC isoforms. *A*, effect of AJH-836 on the level of expression of PKC isoforms in A549 cells. *B*, effect of AJH-836 on the level of expression of PKC isoforms in H358 cells. In *A* and *B*, representative experiments (*top*) and quantification of three independent experiments (*bottom*) are shown. *C*, comparison of 1 μM AJH-836 and 0.1 μM PMA in A549 cells. *D*, comparison of 1 μM AJH-836 and 0.1 μM PMA in H358 cells. Results are expressed as mean ± S.E. (*error bars*) of three individual experiments.

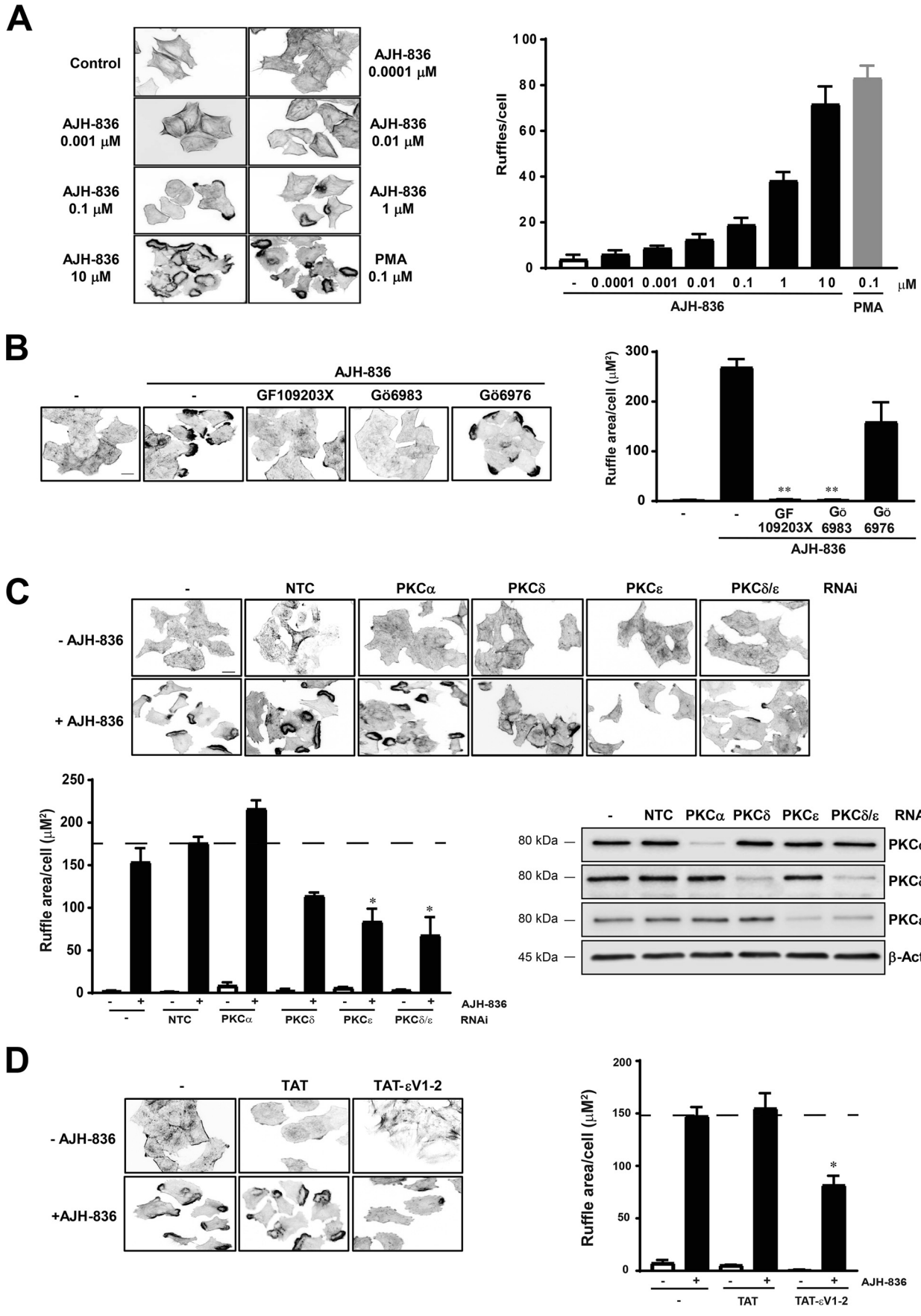
A
Control
AJH-836 0.0001 μM
AJH-836 0.001 μM
AJH-836 0.01 μM
AJH-836 0.1 μM
AJH-836 1 μM
AJH-836 10 μM
PMA 0.1 μM
Ruffles/cell
AJH-836
PMA
μM
B
AJH-836
GF109203X
Gö6983
Gö6976
Ruffle area/cell (μM²)
GF 109203X
Gö 6983
Gö 6976
C
NTC
PKCα
PKCδ
PKCε
PKCδ/ε
RNAi
- AJH-836
+ AJH-836
Ruffle area/cell (μM²)
80 kDa
45 kDa
β-Actin
D
TAT
TAT-εV1-2
- AJH-836
+AJH-836
Ruffle area/cell (μM²)

by C1 domain ligands could promote novel, inhibitory effects on the transformed phenotype. Although we have yet to examine the binding properties of AJH-836 for PKCs expressed in specialized cell types, such as PKCθ (expressed mainly in T lymphocytes) and PKCη (expressed primarily in skin), their homology to PKCδ and PKCϵ, respectively, argues for potential usefulness of this DAG analogue in specific contexts (51, 52).

In summary, the functional characterization of AJH-836 provides a glimpse into the opportunities for PKC isozyme selectivity by manipulation of conformationally constrained DAG-lactones. Given the simplicity and accessibility for chemical modification, this compound provides a platform for the rational design of nPKC-selective agents. Individual members of the PKC family, including nPKCs, and other phorbol ester receptor families have been extensively implicated in human disease, not only cancer but also cardiovascular, neurological, and immunological disorders. Therefore, compounds capable of distinguishing among the different proteins with C1 domains could be promising leads for therapeutic purposes.

Experimental procedures

Cells and reagents

HeLa, A549, and H358 cells were obtained from the ATCC and cultured in DMEM (HeLa cells) or RPMI 1640 medium (A549 and H358 cells) supplemented with 10% FBS, 2 mM glutamine, 100 units/ml penicillin, and 100 μg/ml streptomycin at 37 °C in a humidified 5% CO_2 atmosphere. PMA was purchased from LC Laboratories (Woburn, MA). 4′,6-Diamidino-2-phenylindole (DAPI) was obtained from Roche Diagnostics.

Synthesis of AJH-836 and AJH-1512

The synthesis of AJH-836 and AJH-1512 is reported in detail elsewhere (23). These agents are described as compounds 104 and 98, respectively, in that study.

In vitro binding assays

PKCα, -βII, -δ, and -ϵ were from Life Technologies. Compounds were assayed *in vitro* by competition for the binding of [^{3}H]PDBu (13.5 Ci/mmol; prepared as a custom synthesis by PerkinElmer Life Sciences) in the presence of 100 μg/ml phosphatidylserine and 1 mM EGTA as described previously (5). Incubation was for 5 min at 37 °C. In each competition assay, seven concentrations of ligand (DAG-lactone) were used with the increasing concentrations of ligand spaced at half-log intervals. In each experiment, triplicate measurements at each concentration of ligand were performed. K_i values were calculated from ID_{50} values determined from the competition curves using GraphPad software built-in analysis tools (GraphPad Software, Inc., San Diego, CA).

Translocation of GFP-tagged PKC isozymes in cellular models

For localization studies of GFP-fused PKCs, experiments were carried out essentially as described previously (10). After transfection of cells (5×10^4) with 1 μg of pEGFP-N1-PKCα, pEGFP-N1-PKCδ, or pEGFP-N1-PKCϵ using Lipofectamine 3000, the cells were plated on coverslides in 24-well plates. Twenty-four hours later, cells were serum-starved for 24 h and then stimulated with PMA, AJH-836, AJH-1512, or vehicle for 30 min. After cells were washed with PBS and fixed with precooled (−20 °C, 20 min) methanol, samples were stained with DAPI (1 μg/ml) for 10 min at 4 °C, mounted on a glass slide, and visualized with a Nikon TE2000-U fluorescence microscope. For the quantification of translocated cells, 20–100 cells/plate were visually assessed in a blinded manner. Translocation was also quantitated using ImageJ. A line was traced across the cytoplasm of individual cells, and the signal intensities and profiles were obtained using the Plot profile tool of the program.

Western blotting

Cells were harvested in lysis buffer containing 50 mM Tris-HCl, pH 6.8, 10% glycerol, and 2% β-mercaptoethanol. Cell lysates were subjected to SDS-PAGE and transferred to polyvinylidene difluoride membranes (Millipore Corp.). After being blocked for 1 h with 5% milk or 5% BSA in TBS and 0.1% Tween 20, membranes were incubated overnight with the following primary antibodies: anti-PKCα, anti-PKCδ, anti-PKCϵ (all from Cell Signaling Technology; 1:1,000 dilution; catalogue numbers 2056, 2058, and 2083, respectively), anti-phospho-Ser^{299}-PKCδ (Abcam; 1:1,000 dilution; catalogue number 133456), vinculin (Sigma-Aldrich; 1:5,000; catalogue number V9131), and β-actin (Sigma-Aldrich; 1:50,000 dilution; catalogue number A5441). After extensive washing, membranes were incubated for 1 h with either anti-mouse (1:1,000 dilution) or anti-rabbit (1:3,000 dilution) secondary antibodies conjugated to horseradish peroxidase (Bio-Rad). Bands were visualized and subjected to densitometric analysis using an Odyssey Fc system (LI-COR Biosciences, Lincoln, NE).

PKC down-regulation assays

For assessment of PKC down-regulation, 1.5×10^5 cells were serum-starved for 24 h and then treated with different concentrations of PKC activators. Cells were lysed at different time points (3, 6, 16, and 24 h). Expression of endogenous PKC isozymes was determined by Western blotting.

Cell ruffle formation

Assessment of morphological cytoskeletal changes was done as described before (31). Briefly, A549 lung cancer cells growing on glass coverslides at low confluence were serum-starved for

Figure 6. AJH-836 stimulates the formation of ruffles in lung cancer cells. *A*, A549 cells were serum-starved for 24 h and then stimulated for 30 min with different concentrations of AJH-836 or 0.1 μM PMA as a control. Cells were fixed and stained with phalloidin-rhodamine. *Left*, representative micrographs. *Right*, quantification of cells bearing ruffles, expressed as mean ± S.D. (*error bars*) of five random fields. Similar results were observed in an additional experiment. *B*, effect of different PKC inhibitors (3 μM) on ruffle formation induced by 1 μM AJH-836. *Left*, representative micrographs. *Right*, quantification of ruffle area/cell. *C*, ruffle formation induced by 1 μM AJH-836 in A549 cells subjected to PKCα, PKCδ, and/or PKCϵ RNAi. *NTC*, nontarget control RNAi. *Upper panel*, representative micrographs. *Lower left*, quantification of ruffle area/cell. *Dotted line*, nontarget control RNAi + AJH-836. *Lower right*, representative Western blotting showing specific depletion of PKCs. *D*, ruffle formation induced by 1 μM AJH-836 in the presence of the PKCϵ inhibitor ϵV1-2 or its control TAT peptide. *Left*, representative micrographs. *Right*, quantification of ruffle area/cell. *Dotted line*, parental cells + AJH-836. *B–D*, results are expressed as mean ± S.E. (*error bars*) of 3 independent experiments. *, $p < 0.01$; **, $p < 0.001$.

24 h and stimulated with AJH-836 at the concentrations indicated. Following fixation with 4% formaldehyde, F-actin was stained with phalloidin-rhodamine, and nuclei were counterstained with DAPI. Slides were visualized by fluorescence microscopy, and five random fields were scored for the number of ruffles. Ruffle area was measured by thresholding for signal intensity using ImageJ.

RNAi

For silencing PKC isozymes, we used previously validated ON-TARGETplus RNAi sequences from Dharmacon (Lafayette, CO) as follows: J-003523-17-0002 (PKCα), J-003524-08-0002 (PKCδ), and J-004653-08-0002 (PKCϵ). As a nontarget control, we used D-001810-10 ON-TARGETplus nontargeting siRNA numbers 2 and 5. RNAi duplexes were transfected using Lipofectamine RNAiMAX (Invitrogen). Experiments were carried out 48 h after transfection.

Statistical analysis

Analysis of variance was performed using GraphPad Prism software built-in analysis tools. The confidence interval was set to 95%. A p value <0.05 was considered statistically significant.

Author contributions—M. C., X. Z., M. J. B., P. M. B., and M. G. K. conceptualization; M. C., V. C.-M., R. G., and M. G. K. data curation; M. C., X. Z., V. C.-M., C. L.-H., M. J. B., R. G., P. M. B., and M. G. K. formal analysis; M. C. validation; M. C., X. Z., V. C.-M., C. L.-H., R. G., J. A., P. M. B., and M. G. K. investigation; M. C. and M. G. K. visualization; M. C., X. Z., V. C.-M., C. L.-H., M. J. B., R. G., J. A., J. L., P. M. B., and M. G. K. methodology; M. C., P. M. B., and M. G. K. writing-original draft; J. L., P. M. B., and M. G. K. resources; P. M. B. and M. G. K. funding acquisition; M. G. K. supervision.

References

1. Mellor, H., and Parker, P. J. (1998) The extended protein kinase C superfamily. *Biochem. J.* **332,** 281–292 CrossRef Medline
2. Newton, A. C. (2010) Protein kinase C: poised to signal. *Am. J. Physiol. Endocrinol. Metab.* **298,** E395–E402 CrossRef Medline
3. Griner, E. M., and Kazanietz, M. G. (2007) Protein kinase C and other diacylglycerol effectors in cancer. *Nat. Rev. Cancer* **7,** 281–294 CrossRef Medline
4. Hannun, Y. A., and Bell, R. M. (1986) Phorbol ester binding and activation of protein kinase C on Triton X-100 mixed micelles containing phosphatidylserine. *J. Biol. Chem.* **261,** 9341–9347 Medline
5. Kazanietz, M. G., Krausz, K. W., and Blumberg, P. M. (1992) Differential irreversible insertion of protein kinase C into phospholipid vesicles by phorbol esters and related activators. *J. Biol. Chem.* **267,** 20878–20886 Medline
6. Sharkey, N. A., Leach, K. L., and Blumberg, P. M. (1984) Competitive inhibition by diacylglycerol of specific phorbol ester binding. *Proc. Natl. Acad. Sci. U.S.A.* **81,** 607–610 CrossRef Medline
7. Ono, Y., Fujii, T., Igarashi, K., Kuno, T., Tanaka, C., Kikkawa, U., and Nishizuka, Y. (1989) Phorbol ester binding to protein kinase C requires a cysteine-rich zinc-finger-like sequence. *Proc. Natl. Acad. Sci. U.S.A.* **86,** 4868–4871 CrossRef Medline
8. Zhang, G., Kazanietz, M. G., Blumberg, P. M., and Hurley, J. H. (1995) Crystal structure of the cys2 activator-binding domain of protein kinase Cδ in complex with phorbol ester. *Cell* **81,** 917–924 CrossRef Medline
9. Colón-González, F., and Kazanietz, M. G. (2006) C1 domains exposed: from diacylglycerol binding to protein-protein interactions. *Biochim. Biophys. Acta* **1761,** 827–837 CrossRef Medline
10. von Burstin, V. A., Xiao, L., and Kazanietz, M. G. (2010) Bryostatin 1 inhibits phorbol ester-induced apoptosis in prostate cancer cells by differentially modulating protein kinase C (PKC) δ translocation and preventing PKCδ-mediated release of tumor necrosis factor-α. *Mol. Pharmacol.* **78,** 325–332 CrossRef Medline
11. Wang, Q. J., Bhattacharyya, D., Garfield, S., Nacro, K., Marquez, V. E., and Blumberg, P. M. (1999) Differential localization of protein kinase Cδ by phorbol esters and related compounds using a fusion protein with green fluorescent protein. *J. Biol. Chem.* **274,** 37233–37239 CrossRef Medline
12. Cooke, M., Magimaidas, A., Casado-Medrano, V., and Kazanietz, M. G. (2017) Protein kinase C in cancer: the top five unanswered questions. *Mol. Carcinog.* **56,** 1531–1542 CrossRef Medline
13. Mischak, H., Goodnight, J. A., Kolch, W., Martiny-Baron, G., Schaechtle, C., Kazanietz, M. G., Blumberg, P. M., Pierce, J. H., and Mushinski, J. F. (1993) Overexpression of protein kinase C-δ and -ϵ in NIH 3T3 cells induces opposite effects on growth, morphology, anchorage dependence, and tumorigenicity. *J. Biol. Chem.* **268,** 6090–6096 Medline
14. Szallasi, Z., Krsmanovic, L., and Blumberg, P. M. (1993) Nonpromoting 12-deoxyphorbol 13-esters inhibit phorbol 12-myristate 13-acetate induced tumor promotion in CD-1 mouse skin. *Cancer Res.* **53,** 2507–2512 Medline
15. Hennings, H., Blumberg, P. M., Pettit, G. R., Herald, C. L., Shores, R., and Yuspa, S. H. (1987) Bryostatin 1, an activator of protein kinase C, inhibits tumor promotion by phorbol esters in SENCAR mouse skin. *Carcinogenesis* **8,** 1343–1346 CrossRef Medline
16. Bocklandt, S., Blumberg, P. M., and Hamer, D. H. (2003) Activation of latent HIV-1 expression by the potent anti-tumor promoter 12-deoxyphorbol 13-phenylacetate. *Antiviral Res.* **59,** 89–98 CrossRef Medline
17. Russo, P., Kisialiou, A., Lamonaca, P., Moroni, R., Prinzi, G., and Fini, M. (2015) New drugs from marine organisms in Alzheimer's disease. *Mar. Drugs* **14,** 5 CrossRef Medline
18. Mochly-Rosen, D., Das, K., and Grimes, K. V. (2012) Protein kinase C, an elusive therapeutic target? *Nat. Rev. Drug Discov.* **11,** 937–957 CrossRef Medline
19. Blumberg, P. M., Kedei, N., Lewin, N. E., Yang, D., Czifra, G., Pu, Y., Peach, M. L., and Marquez, V. E. (2008) Wealth of opportunity—the C1 domain as a target for drug development. *Curr. Drug Targets* **9,** 641–652 CrossRef Medline
20. Pu, Y., Perry, N. A., Yang, D., Lewin, N. E., Kedei, N., Braun, D. C., Choi, S. H., Blumberg, P. M., Garfield, S. H., Stone, J. C., Duan, D., and Marquez, V. E. (2005) A novel diacylglycerol-lactone shows marked selectivity *in vitro* among C1 domains of protein kinase C (PKC) isoforms α and δ as well as selectivity for RasGRP compared with PKCα. *J. Biol. Chem.* **280,** 27329–27338 CrossRef Medline
21. Marquez, V. E., and Blumberg, P. M. (2003) Synthetic diacylglycerols (DAG) and DAG-lactones as activators of protein kinase C (PK-C). *Acc. Chem. Res.* **36,** 434–443 CrossRef Medline
22. Garcia-Bermejo, M. L., Leskow, F. C., Fujii, T., Wang, Q., Blumberg, P. M., Ohba, M., Kuroki, T., Han, K. C., Lee, J., Marquez, V. E., and Kazanietz, M. G. (2002) Diacylglycerol (DAG)-lactones, a new class of protein kinase C (PKC) agonists, induce apoptosis in LNCaP prostate cancer cells by selective activation of PKCα. *J. Biol. Chem.* **277,** 645–655 CrossRef Medline
23. Nacro, K., Bienfait, B., Lee, J., Han, K. C., Kang, J. H., Benzaria, S., Lewin, N. E., Bhattacharyya, D. K., Blumberg, P. M., and Marquez, V. E. (2000) Conformationally constrained analogues of diacylglycerol (DAG). 16. How much structural complexity is necessary for recognition and high binding affinity to protein kinase C? *J. Med. Chem.* **43,** 921–944 CrossRef Medline
24. Duan, D., Sigano, D. M., Kelley, J. A., Lai, C. C., Lewin, N. E., Kedei, N., Peach, M. L., Lee, J., Abeyweera, T. P., Rotenberg, S. A., Kim, H., Kim, Y. H., El Kazzouli, S., Chung, J. U., Young, H. A., *et al.* (2008) Conformationally constrained analogues of diacylglycerol. 29. Cells sort diacylglycerol-lactone chemical zip codes to produce diverse and selective biological activities. *J. Med. Chem.* **51,** 5198–5220 CrossRef Medline
25. Kazanietz, M. G., Areces, L. B., Bahador, A., Mischak, H., Goodnight, J., Mushinski, J. F., and Blumberg, P. M. (1993) Characterization of ligand

and substrate specificity for the calcium-dependent and calcium-independent protein kinase C isozymes. *Mol. Pharmacol.* **44,** 298–307 Medline
26. Ann, J., Yoon, S., Baek, J., Kim, D. H., Lewin, N. E., Hill, C. S., Blumberg, P. M., and Lee, J. (2015) Design and synthesis of protein kinase Cε selective diacylglycerol lactones (DAG-lactones). *Eur. J. Med. Chem.* **90,** 332–341 CrossRef Medline
27. Garg, R., Benedetti, L. G., Abera, M. B., Wang, H., Abba, M., and Kazanietz, M. G. (2014) Protein kinase C and cancer: what we know and what we do not. *Oncogene* **33,** 5225–5237 CrossRef Medline
28. Basu, A., and Sivaprasad, U. (2007) Protein kinase Cε makes the life and death decision. *Cell. Signal.* **19,** 1633–1642 CrossRef Medline
29. Gorin, M. A., and Pan, Q. (2009) Protein kinase Cε: an oncogene and emerging tumor biomarker. *Mol Cancer.* **8,** 9 CrossRef Medline
30. Caino, M. C., Lopez-Haber, C., Kim, J., Mochly-Rosen, D., and Kazanietz, M. G. (2012) Protein kinase Cε is required for non-small cell lung carcinoma growth and regulates the expression of apoptotic genes. *Oncogene* **31,** 2593–2600 CrossRef Medline
31. Caino, M. C., Lopez-Haber, C., Kissil, J. L., and Kazanietz, M. G. (2012) Non-small cell lung carcinoma cell motility, rac activation and metastatic dissemination are mediated by protein kinase Cε. *PLoS One* **7,** e31714 CrossRef Medline
32. Garg, R., Blando, J. M., Perez, C. J., Abba, M. C., Benavides, F., and Kazanietz, M. G. (2017) Protein kinase Cε cooperates with PTEN loss for prostate tumorigenesis through the CXCL13-CXCR5 pathway. *Cell Rep.* **19,** 375–388 CrossRef Medline
33. Kim, H., Na, Y. R., Kim, S. Y., and Yang, E. G. (2016) Protein kinase C isoforms differentially regulate hypoxia-inducible factor-1α accumulation in cancer cells. *J. Cell. Biochem.* **117,** 647–658 CrossRef Medline
34. Kajimoto, T., Shirai, Y., Sakai, N., Yamamoto, T., Matsuzaki, H., Kikkawa, U., and Saito, N. (2004) Ceramide-induced apoptosis by translocation, phosphorylation, and activation of protein kinase Cδ in the Golgi complex. *J. Biol. Chem.* **279,** 12668–12676 CrossRef Medline
35. Wang, H., Xiao, L., and Kazanietz, M. G. (2011) p23/Tmp21 associates with protein kinase Cδ (PKCδ) and modulates its apoptotic function. *J. Biol. Chem.* **286,** 15821–15831 CrossRef Medline
36. Okhrimenko, H., Lu, W., Xiang, C., Ju, D., Blumberg, P. M., Gomel, R., Kazimirsky, G., and Brodie, C. (2005) Roles of tyrosine phosphorylation and cleavage of protein kinase Cδ in its protective effect against tumor necrosis factor-related apoptosis inducing ligand-induced apoptosis. *J. Biol. Chem.* **280,** 23643–23652 CrossRef Medline
37. Durgan, J., Michael, N., Totty, N., and Parker, P. J. (2007) Novel phosphorylation site markers of protein kinase Cδ activation. *FEBS Lett.* **581,** 3377–3381 CrossRef Medline
38. Kedei, N., Chen, J. Q., Herrmann, M. A., Telek, A., Goldsmith, P. K., Petersen, M. E., Keck, G. E., and Blumberg, P. M. (2014) Molecular systems pharmacology: isoelectric focusing signature of protein kinase Cδ provides an integrated measure of its modulation in response to ligands. *J. Med. Chem.* **57,** 5356–5369 CrossRef Medline
39. Olivier, A. R., and Parker, P. J. (1992) Identification of multiple PKC isoforms in Swiss 3T3 cells: differential down-regulation by phorbol ester. *J. Cell. Physiol.* **152,** 240–244 CrossRef Medline
40. Parker, P. J., Bosca, L., Dekker, L., Goode, N. T., Hajibagheri, N., and Hansra, G. (1995) Protein kinase C (PKC)-induced PKC degradation: a model for down-regulation. *Biochem. Soc. Trans.* **23,** 153–155 CrossRef Medline
41. Lum, M. A., Pundt, K. E., Paluch, B. E., Black, A. R., and Black, J. D. (2013) Agonist-induced down-regulation of endogenous protein kinase Cα through an endolysosomal mechanism. *J. Biol. Chem.* **288,** 13093–13109 CrossRef Medline
42. Ridley, A. J. (2015) Rho GTPase signalling in cell migration. *Curr. Opin. Cell Biol.* **36,** 103–112 CrossRef Medline
43. Kazanietz, M. G., and Caloca, M. J. (2017) The Rac GTPase in cancer: from old concepts to new paradigms. *Cancer Res.* **77,** 5445–5451 CrossRef Medline
44. Martiny-Baron, G., Kazanietz, M. G., Mischak, H., Blumberg, P. M., Kochs, G., Hug, H., Marmé, D., and Schächtele, C. (1993) Selective inhibition of protein kinase C isozymes by the indolocarbazole Gö 6976. *J. Biol. Chem.* **268,** 9194–9197 Medline
45. Begley, R., Liron, T., Baryza, J., and Mochly-Rosen, D. (2004) Biodistribution of intracellularly acting peptides conjugated reversibly to Tat. *Biochem. Biophys. Res. Commun.* **318,** 949–954 CrossRef Medline
46. Ohashi, N., Kobayashi, R., Nomura, W., Kobayakawa, T., Czikora, A., Herold, B. K., Lewin, N. E., Blumberg, P. M., and Tamamura, H. (2017) Synthesis and evaluation of dimeric derivatives of diacylglycerol-lactones as protein kinase C ligands. *Bioconjug. Chem.* **28,** 2135–2144 CrossRef Medline
47. Bögi, K., Lorenzo, P. S., Szállási, Z., Acs, P., Wagner, G. S., and Blumberg, P. M. (1998) Differential selectivity of ligands for the C1a and C1b phorbol ester binding domains of protein kinase Cδ: possible correlation with tumor-promoting activity. *Cancer Res.* **58,** 1423–1428 Medline
48. Pu, Y., Garfield, S. H., Kedei, N., and Blumberg, P. M. (2009) Characterization of the differential roles of the twin C1a and C1b domains of protein kinase C-δ. *J. Biol. Chem.* **284,** 1302–1312 CrossRef Medline
49. Garcia, L. C., Donadío, L. G., Mann, E., Kolusheva, S., Kedei, N., Lewin, N. E., Hill, C. S., Kelsey, J. S., Yang, J., Esch, T. E., Santos, M., Peach, M. L., Kelley, J. A., Blumberg, P. M., Jelinek, R., *et al.* (2014) Synthesis, biological, and biophysical studies of DAG-indololactones designed as selective activators of RasGRP. *Bioorg. Med. Chem.* **22,** 3123–3140 CrossRef Medline
50. Elhalem, E., Donadío, L. G., Zhou, X., Lewin, N. E., Garcia, L. C., Lai, C. C., Kelley, J. A., Peach, M. L., Blumberg, P. M., and Comin, M. J. (2017) Exploring the influence of indololactone structure on selectivity for binding to the C1 domains of PKCα, PKCε, and RasGRP. *Bioorg. Med. Chem.* **25,** 2971–2980 CrossRef Medline
51. Hayashi, K., and Altman, A. (2007) Protein kinase Cθ (PKCθ): a key player in T cell life and death. *Pharmacol. Res.* **55,** 537–544 CrossRef Medline
52. Kashiwagi, M., Ohba, M., Chida, K., and Kuroki, T. (2002) Protein kinase Cη (PKCη): its involvement in keratinocyte differentiation. *J. Biochem.* **132,** 853–857 CrossRef Medline